

Effects of elevated $p\text{CO}_2$ on physiological performance of marine microalgae *Dunaliella salina* (Chlorophyta, Chlorophyceae)*

HU Shunxin (胡顺鑫)¹, WANG You (王悠)¹, WANG Ying (王影)¹, ZHAO Yan (赵妍)¹, ZHANG Xinxin (张鑫鑫)¹, ZHANG Yongsheng (张永生)^{1,2}, JIANG Ming (姜铭)¹, TANG Xuexi (唐学玺)^{1,**}

¹ College of Marine Life Science, Ocean University of China, Qingdao 266003, China

² Rongcheng Ocean and Fisheries Bureau, Weihai 264300, China

Received Oct. 8, 2016; accepted in principle Dec. 2, 2016; accepted for publication Feb. 3, 2017

© Chinese Society for Oceanology and Limnology, Science Press and Springer-Verlag GmbH Germany, part of Springer Nature 2018

Abstract The present study was conducted to determine the effects of elevated $p\text{CO}_2$ on growth, photosynthesis, dark respiration and inorganic carbon acquisition in the marine microalga *Dunaliella salina*. To accomplish this, *D. salina* was incubated in semi-continuous cultures under present-day CO_2 levels (390 μatm , pH_{NBS} : 8.10), predicted year 2100 CO_2 levels (1 000 μatm , pH_{NBS} : 7.78) and predicted year 2300 CO_2 levels (2 000 μatm , pH_{NBS} : 7.49). Elevated $p\text{CO}_2$ significantly enhanced photosynthesis (in terms of gross photosynthetic O_2 evolution, effective quantum yield ($\Delta F/F'_m$), photosynthetic efficiency (α), maximum relative electron transport rate ($r\text{ETR}_{\text{max}}$) and ribulose-1,5-bisphosphate carboxylase/oxygenase (Rubisco) activity) and dark respiration of *D. salina*, but had insignificant effects on growth. The photosynthetic O_2 evolution of *D. salina* was significantly inhibited by the inhibitors acetazolamide (AZ), ethoxymolamide (EZ) and 4,4'-diisothiocyano-stilbene-2,2'-disulfonate (DIDS), indicating that *D. salina* is capable of acquiring HCO_3^- via extracellular carbonic anhydrase and anion-exchange proteins. Furthermore, the lower inhibition of the photosynthetic O_2 evolution at high $p\text{CO}_2$ levels by AZ, EZ and DIDS and the decreased carbonic anhydrase showed that carbon concentrating mechanisms were down-regulated at high $p\text{CO}_2$. In conclusion, our results show that photosynthesis, dark respiration and CCMs will be affected by the increased $p\text{CO}_2$ /low pH conditions predicted for the future, but that the responses of *D. salina* to high $p\text{CO}_2$ /low pH might be modulated by other environmental factors such as light, nutrients and temperature. Therefore, further studies are needed to determine the interactive effects of $p\text{CO}_2$, temperature, light and nutrients on marine microalgae.

Keyword: ocean acidification; growth; photosynthesis; CO_2 ; CCMs; *Dunaliella salina*

1 INTRODUCTION

The concentration of atmospheric CO_2 has increased from ~280 to 395 μatm since the Industrial Revolution because of human activities such as deforestation, cement manufacture and burning of fossil fuels (Caldeira and Wickett, 2003). As humans continue to burn fossil fuels and biomass, atmospheric $p\text{CO}_2$ is predicted to continue to increase by a minimum of 0.5% per year in the next centuries, reaching 1 000 and 2 000 μatm by 2100 and 2300, respectively (Caldeira and Wickett, 2003; IPCC, 2013). Approximately 1/3 of this atmospheric $p\text{CO}_2$

will be dissolved in the surface ocean, increasing CO_2 (aq) and decreasing the pH, thereby changing the seawater carbonate chemistry in a process called ocean acidification (Guinotte and Fabry, 2008). By 2100 and 2300, oceanic absorption of CO_2 will lead to a decrease in pH of 0.4 and 0.7 pH units, respectively (Caldeira and Wickett, 2003).

* Supported by the Joint Funds of the National Natural Science Foundation of China and the Marine Science Research Center of the People's Government of Shandong Province (No. U1406403) and the National Natural Science Foundation of China (No. 41476091)

** Corresponding author: tangxx@ouc.edu.cn

Marine algae fix inorganic carbon via the enzyme ribulose-1,5-bisphosphate carboxylase/oxygenase (RubisCO), which utilizes CO_2 exclusively as the substrate for the carboxylase reaction. The concentration of $\text{CO}_{2(\text{aq})}$ ($\sim 10 \mu\text{mol/L}$) in oceans at present is far less than the half-saturation constant of RubisCO ($\sim 20\text{--}200 \mu\text{mol/L}$) (Badger et al., 1998). Consequently, most marine algae have developed CO_2 concentrating mechanisms (CCMs) to overcome the limitations of RubisCO and compensate for the low $\text{CO}_{2(\text{aq})}$ (Rost et al., 2006). Marine algae have evolved diverse types of CCMs, two of which are widely found. In the first CCM, the reversible dehydration of HCO_3^- to CO_2 is catalyzed by extracellular carbonic anhydrase at the cell surface, then taken into the cell by passive diffusion, while in the second, HCO_3^- is transported across cell membranes via anion exchange (AE), after which CO_2 is produced through the dehydration of HCO_3^- catalyzed by intracellular carbonic anhydrase (Reinfelder, 2011). The types and energy costs of CCMs will largely determine the sensitivity of marine algae to ocean acidification (Reinfelder, 2011).

Functioning of CCMs has been widely investigated in different algal species. In diatoms, the CCMs of *Pseudo-nitzschia multiseries*, *Stellarima stellaris*, *Phaeodactylum tricornutum* and *Thalassiosira pseudonana* were down-regulated with elevated $p\text{CO}_2$, as indicated by reduced photosynthetic affinities for dissolved inorganic carbon (DIC) and CO_2 (Trimborn et al., 2008; Wu et al., 2010; Yang and Gao, 2012). Furthermore, these responses were generally accompanied by reduced active transport of HCO_3^- or lowered extracellular carbonic anhydrase activities. The affinities for CO_2 and DIC were also lower under high $p\text{CO}_2$ conditions in the coccolithophore *Emiliania huxleyi* and the cyanobacterium *Trichodesmium*, while CA_{ext} activity appeared to play a minor role in CCMs, and was not affected by elevated $p\text{CO}_2$ (Rost et al., 2003, Kranz et al., 2009). Furthermore, the relative expression of genes associated with carbonic anhydrases and aquaporins in the dinoflagellate *Thoracosphaera heimii* decreased with increasing $p\text{CO}_2$ (Van de Waal et al., 2013). Nevertheless, Zou and Gao (2009) and Zou et al. (2011) reported that *Hizikia fusiformis* and *Gracilaria lemaneiformis* showed no down-regulation of CCMs with elevated $p\text{CO}_2$. These different types of CCMs and their responses to ocean acidification have deepened our knowledge of species-specific responses to ocean acidification in marine algae.

Inevitably, the expression and operation of CCMs involve an energetic investment. Down-regulation under high CO_2 conditions could reduce the energetic requirement for photosynthesis. Consequently, the energy saved from down-regulated CCMs could be invested in other physiological processes, such as assimilation of other nutrients, leading to stimulated growth and photosynthesis (Giordano et al., 2005; Riebesell et al., 2007; Wu et al., 2010). Nevertheless, elevated $p\text{CO}_2$ is not always beneficial to marine algae. It has been widely reported that calcifying organisms are more sensitive to ocean acidification due to the negative effects they have on the formation of aragonite or calcite armor (Langer et al., 2006; Kurihara et al., 2008; Van de Waal et al., 2013), while negative effects on growth and photosynthesis have been observed in non-calcifying species (Mercado et al., 1999; Iñíguez et al., 2015), likely due to the negative effects on the physiological processes caused by reduced external pH.

Dunaliella salina is a unicellular and halotolerant biflagellate marine microalgal species that has been widely applied as an important model organism to evaluate physiological responses to environmental changes and fundamental molecular mechanisms because of its tolerance to hyper salinity and the simplicity of its cytoarchitecture (Booth and Beardall, 1991; Zhang et al., 2015). However, comprehensive studies of the effects of elevated $p\text{CO}_2$ on the physiological performance of this species remain scarce. Nevertheless, it is essential to investigate the long-term acclimation of physiological activities such as photosynthesis and respiration under stable carbonate chemistry. Therefore, our study was conducted using semi-continuous cultures to maintain stable carbonate chemistry systems while keeping the microalgae in an exponential stage for a long period of time. The specific goal of this study was to improve our understanding of the physiological responses of the marine microalgae *D. salina* to elevated $p\text{CO}_2$. This was achieved by evaluating the growth, photosynthesis, dark respiration and CCM modes of *D. salina* under three different $p\text{CO}_2$ levels in semi-continuous cultures. The three $p\text{CO}_2$ levels included: $390 \mu\text{atm}$ (pH_{NBS} : 8.10), which is the present pH value, as well as $1\,000 \mu\text{atm}$ (pH_{NBS} : 7.78) and $p\text{CO}_2$: $2\,000 \mu\text{atm}$ (pH_{NBS} : 7.49), which are the pH values predicted for 2100 and 2300, respectively. We hypothesized that CO_2 -induced ocean acidification will change the metabolic energy requirement to balance the reduced external pH, and that elevated

CO₂ availability and changes in seawater carbonate chemistry may reduce their ability to actively transport CO₂ and HCO₃⁻, thereby reducing the energetic costs of CCMs. Consequently, these effects are predicted to lead to different physiological sensitivities to CO₂-induced ocean acidification.

2 MATERIAL AND METHOD

2.1 Culture conditions and experimental design

D. salina was obtained from the Culture Collection of Algae at the Ocean University of China. The cells were cultured in 0.45 µm-filtered natural seawater collected from Lu Xun seaside Park (Qingdao), which had been autoclaved (30 min, 121°C) and enriched with modified f/2 medium (Guillard, 1975). All cultures were incubated at 20±1°C and illuminated with 80 µmol photon/(m²·s) (a sub-saturating light intensity) under a 12 h:12 h light: dark cycle. The salinity of the culture medium was adjusted to 30.

Experiments were conducted in triplicate in 500 mL sterilized and acid-washed Erlenmeyer flasks containing 300 mL medium. Prior to inoculation, the cultures were aerated with three different CO₂ levels: 390, 1 000 and 2 000 µatm, corresponding to approximately present-day levels and those predicted for 2100 and 2300, respectively. Different air/CO₂ mixtures were generated by plant CO₂ chambers (HP400G-D, Ruihua Instrument & Equipment Ltd., Wuhan, China) with a variation of less than 5%. Semi-continuous cultures used to measure the physiological responses of *D. salina* to elevated *p*CO₂ in the present study have been widely applied in other relevant studies (Fu et al., 2007; Hutchins et al., 2007; Wu et al., 2010). In the present study the culture medium was renewed every 24 h to ensure that the cell concentration remained within a range of 2×10⁴ to 5×10⁴ cells/mL (the dilution rate is about 40%) at their exponential growth phase so that the pH fluctuations during growth were less than 0.06. Cultures were harvested following 4–6 weeks of semi-continuous incubation when their growth rates did not fluctuate significantly for three or more consecutive days, at which time they were considered fully acclimated to their respective experimental treatments.

2.2 Seawater carbonate chemistry

The concentrations of dissolved inorganic carbon (DIC) and pH were measured before and after diluting the culture, as well as during the middle of the light

period to ensure stability of the carbonate system in culture. The DIC was determined using a total organic carbon analyzer (TOC-V_{CPN}, Shimadzu) following the method described by Liu et al. (2014). pH values were determined using a pH meter (SevenCompact™ S210k, METTLER TOLEDO) calibrated with the standard National Bureau of Standards (NBS) buffer system in a three-point calibration. The other relevant parameters of the seawater carbonate system were computed according to the known values of pH, DIC, salinity, temperature and *p*CO₂ using the CO₂SYS software (Lewis et al., 1998).

2.3 Growth and photosynthetic pigment

The growth rate of microalgae was monitored daily using a hemocytometer before and after the medium was renewed. The specific growth rate (μ) was calculated from the equation: $\mu = (\ln N_1 - \ln N_0) / (t_1 - t_0)$, where N_0 and N_1 represent the average cell numbers at times t_0 (initial or just after the dilution) and t_1 (before the dilution), respectively.

Chlorophyll *a* (Chl *a*), chlorophyll *b* (Chl *b*) and carotenoid (*Car*) concentrations were measured according to Wellburn (1994). Briefly, 60 mL of culture were filtered onto glass microfiber filters (GF/F, Whatman), then extracted with 10 mL of methanol overnight at 4°C. Concentrations were calculated according to the following equations:

$$\text{Chl } a \text{ (}\mu\text{g/L)} = 16.72 A_{665} - 9.16 A_{652},$$

$$\text{Chl } b \text{ (}\mu\text{g/L)} = 34.09 A_{652} - 15.28 A_{665},$$

$$\text{Car (}\mu\text{g/L)} = (1000 A_{470} - 1.63 \text{ Chl } a - 104.96 \text{ Chl } b) / 221,$$

where, A_{470} , A_{652} and A_{665} represent absorbance values of the acetone extracts at 470 nm, 652 nm and 665 nm, respectively.

2.4 Chlorophyll fluorescence measurements

Fluorescence induction curves and rapid light curves (RLCs) were applied to evaluate the changes in photosynthetic performance of microalgae under different levels of *p*CO₂ using a pulse amplitude-modulated fluorometer (Water-PAM fluorometer, Walz, Effeltrich, Germany).

The RLCs were determined at eight different PAR levels (83, 123, 188, 282, 400, 556, 991 and 1 332 µmol photon/(m²·s)), each of which lasted 10s. The RLCs were fitted with the empirical equation proposed by Platt et al. (1980) to determine the relevant parameters; namely, rETR_{max} (maximum relative electron transport rate), α (photosynthetic efficiency), and E_k (light saturation point). The

minimum saturating irradiation was derived from $rETR_{max}$ and α according to the following equation: $E_k = rETR_{max}/\alpha$. The following settings ensured convergence of the regression model: iterations=100, step size=100, tolerance=0.000 1, and initial seed value for $P=5$, $\alpha=0.05$ and $\beta=0$ (Ralph and Gademann, 2005).

For fluorescence induction curves, all of the samples were dark-adapted for 20 min before measurement. The dark-adapted induction curves were then measured with a delay of 40 s between F_v/F_m measurements. The actinic light was set at $188 \mu\text{mol photon}/(\text{m}^2 \cdot \text{s})$ to measure the value of effective quantum yield ($\Delta F/F'_m$) and non-photochemical quenching (NPQ).

2.5 Photosynthetic oxygen evolution and respiration

Photosynthetic oxygen evolution and dark respiration were measured using a Clark-type oxygen electrode (Chlorolab 3, Hansatech, UK). Light was supplied by a halogen lamp, and temperature was maintained using a water bath circulator at 20°C . Prior to the determinations, the cells were allowed to acclimate to the light or dark conditions in the reaction chamber for 15 min. The 5 mL reaction medium was continuously magnetically stirred during the measurement.

The evolution of photosynthetic oxygen of *D. salina* under different $p\text{CO}_2$ values with the addition of inhibitors was measured to determine the mechanism of inorganic carbon acquisition. The inhibitors included acetazolamide (AZ), which is an impermeant CA inhibitor and thus inhibits only extracellular CA, ethoxzolamide (EZ), which is a membrane-permeable carbonic anhydrase inhibitor that can inhibit both extracellular and intracellular CA, and DIDS (4,4'-diisothiocyanostilbene-2,2'-disulfonate), which inhibits direct HCO_3^- uptake by means of the anion-exchange protein. These inhibitors have been widely used to determine the contribution of external CA, internal CA and anion-exchange protein to photosynthetic inorganic carbon uptake (Moroney et al., 1985; Axelsson et al., 1995; Ihnken et al., 2011).

2.6 Determination of ribulose-1,5-bisphosphate carboxylase/oxygenase (Rubisco) activities

The cells were collected by centrifugation at $3\ 000 \times g$ and 4°C for 15 min. After removing the supernatant, 1 mL buffer solution (40 mmol/L Tris-

HCl, 5 mmol/L glutathione, 10 mmol/L MgCl_2 and 0.25 mmol/L EDTA, pH 7.6) was added, and the cells were ground on ice. The liquid was subsequently concentrated, after which the supernatant was used for further assays. The Rubisco activity in the supernatant was generally determined following the methods described by Gerard and Driscoll (1996). Briefly, the assay mixture contained 5 mmol/L NADH, 50 mmol/L ATP, 50 mmol/L phosphocreatine, 0.2 mmol/L NaHCO_3 , 160 U/mL creatine phosphokinase, 160 U/mL phosphoglycerate kinase, 160 U/mL glyceraldehyde-3-phosphate dehydrogenase and reaction buffer (0.1 mol/L Tris-HCl, 12 mmol/L MgCl_2 and 0.4 mmol/L EDTA, pH 7.8). The absorbance values at 340 nm (A_{340}) were measured every 20 s for 3 min to obtain the background NADH oxidation rate. Next, 0.05 mL RuBP (final concentration of 25 mmol/L) was added into the assay mixture, and the A_{340} was recorded every 20 s for 3 min. The activities of Rubisco were computed by subtracting the background rate of decrease in A_{340} from the rate determined in the three minutes following RuBP addition and then converting the corrected rate of A_{340} decrease to a rate of NADH oxidation.

2.7 Measurement of carbonic anhydrase activity

Cells grown under three different $p\text{CO}_2$ levels were collected to determine the internal carbonic anhydrase and external carbonic anhydrase activity according to an electrometric method (Giordano and Maberly, 1989). Briefly, cells were harvested by centrifugation at $4\ 000 \times g$ and 4°C for 10 min, then re-suspended in Veronal buffer (20 mmol/L, pH 8.2) adjusted to the salinity of the culture medium with NaCl. The cell suspension was initially analyzed for CA_{ext} activity, after which it was used for CA_{int} determination. The CA_{ext} was determined based on the time taken for the pH to decrease from 8.2 to 7.2 following the addition of 2 mL CO_2 -saturated distilled water (also adjusted to the salinity of the culture medium with NaCl) to a 5 mL cell suspension. For measurements of CA_{int} activity, the same method as described above was used; however, the cell suspension was disrupted by a sonicator and the disruption of cells was confirmed by microscopic observation. Enzyme activity was calculated using the following equation:

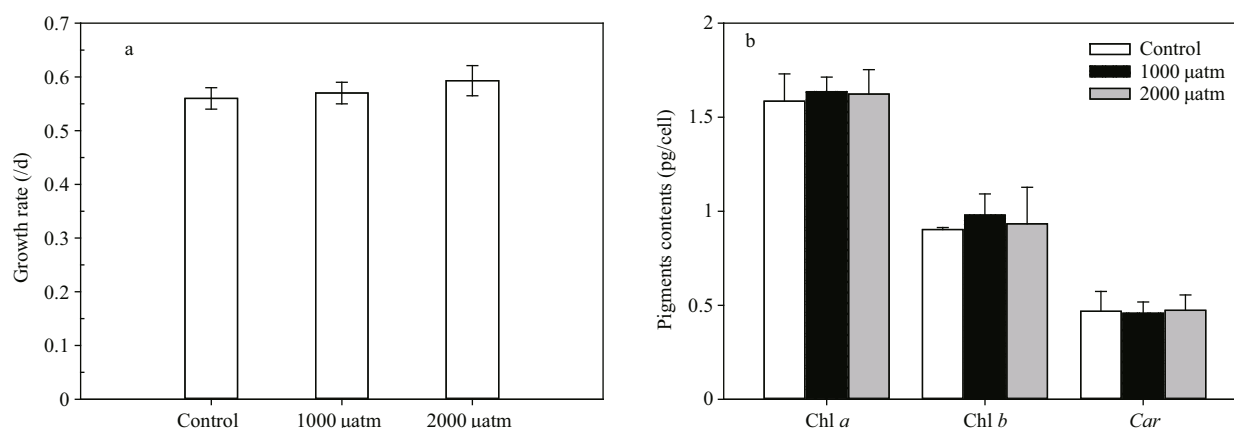
$$EU = 10(T_0/T - 1),$$

where, T_0 is the uncatalyzed reaction and T is the time of the catalyzed reaction.

Table 1 Parameters of the seawater carbonate chemistry system at different $p\text{CO}_2$ levels prior to and after dilution

		pH_{NBS}	DIC ($\mu\text{mol/kg}$)	HCO_3^- ($\mu\text{mol/kg}$)	CO_3^{2-} ($\mu\text{mol/kg}$)	CO_2 ($\mu\text{mol/kg}$)	TA ($\mu\text{mol/kg}$)
Control	Prior	8.12 \pm 0.02 ^a	1 925.6 \pm 13.0 ^a	1 760.8 \pm 4.1 ^a	146.3 \pm 6.5 ^a	14.1 \pm 0.8 ^a	2 100.6 \pm 15.0 ^a
	After	8.10 \pm 0.01 ^a	1 900.0 \pm 11.6 ^a	1 752.4 \pm 6.3 ^a	132.1 \pm 2.5 ^a	15.4 \pm 0.2 ^a	2 079.3 \pm 25.6 ^a
1 000 μatm	Prior	7.81 \pm 0.01 ^b	2 013.3 \pm 17.0 ^b	1 906.9 \pm 15.2 ^b	73.6 \pm 2.4 ^b	32.7 \pm 0.6 ^b	2 089.1 \pm 20.5 ^a
	After	7.77 \pm 0.02 ^b	1 992.6 \pm 6.0 ^b	1 889.4 \pm 5.0 ^b	68.9 \pm 1.7 ^b	34.3 \pm 0.8 ^b	2 080.4 \pm 19.1 ^a
2 000 μatm	Prior	7.52 \pm 0.01 ^c	2 137.2 \pm 14.7 ^c	2 029.4 \pm 14.5 ^c	40.8 \pm 1.1 ^c	66.9 \pm 0.9 ^c	2 130.1 \pm 17.1 ^a
	After	7.49 \pm 0.02 ^c	2 110.6 \pm 11.3 ^c	2 002.9 \pm 11.5 ^c	38.3 \pm 1.3 ^c	69.4 \pm 1.6 ^c	2 110.6 \pm 11.3 ^a

The dissolved inorganic carbon (DIC) concentration, pH_{NBS} , temperature and salinity were used to compute other parameters with the CO_2 system analyzing software (CO2SYS). Data are shown as the means \pm SE ($n=3$). Different superscripted letters represent significant difference among the data.

**Fig.1** The growth rate (a) and pigment contents (chlorophyll *a*, chlorophyll *b* and carotenoids) (b) of *D. salina* acclimated to different $p\text{CO}_2$ levels

Data shown are the means \pm SE ($n=9$).

3 STATISTICAL ANALYSIS

One-way ANOVA was conducted to identify significant differences among treatments using the SPSS software (20.0). The LSD (Least Significant Difference) post-hoc comparison test was used if ANOVA indicated a significant difference. Prior to analysis, data were initially examined for normality using the Shapiro-Wilk test and for homogeneity of variances using Levene's test. Dates were presented as the means \pm SE and the significance was set to $P<0.05$. All figures were prepared with Sigmaplot 12.5.

4 RESULT

4.1 Carbonate system

Under the simulated laboratory conditions of ocean acidification, the seawater carbonate chemistry system under high $p\text{CO}_2$ (1 000 μatm and 2 000 μatm) levels showed significant changes compared to under 390 μatm CO_2 conditions (Table 1). Throughout the semi-continuous culture systems, the pH varied by less than 0.04 before and after diluting the culture medium.

4.2 Growth and photosynthetic pigment

The growth rates of *D. salina* at three different $p\text{CO}_2$ treatments were 0.56 \pm 0.02, 0.57 \pm 0.02 and 0.59 \pm 0.03, respectively (Fig.1a). However, the growth rates of *D. salina* did not vary significantly ($P>0.05$) among $p\text{CO}_2$ treatments. Similar to the growth rates, elevated $p\text{CO}_2$ had no significant ($P>0.05$) effect on the concentrations of chlorophyll *a*, chlorophyll *b* and carotenoids (Fig.1b).

4.3 Chlorophyll fluorescence

The rapid light curves (RLCs) of *D. salina* acclimated to different $p\text{CO}_2$ levels showed a classical pattern of rETR as a function of PAR (Fig.2). With regard to the parameters derived from the RLCs (Table 2), the α value increased significantly by 13.4% ($P<0.01$) and 10.5% ($P<0.01$) when exposed to 1 000 and 2 000 μatm $p\text{CO}_2$, respectively. Similar to the trend in α , the rETR_{max} increased significantly by 20.4% ($P<0.05$) and 27.5% ($P<0.01$) when exposed to 1 000 and 2 000 μatm CO_2 , respectively. In addition, the E_k value under 2 000 μatm CO_2 was significantly higher than that of the control ($P<0.01$), while there

was no significant difference between 390 μatm and 1 000 μatm CO_2 ($P>0.05$). Neither elevated $p\text{CO}_2$ conditions significantly influenced the value of β ($P>0.05$).

The $\Delta F/F'_m$ value during the induction curves (Fig.3a) showed that elevated $p\text{CO}_2$ increased the effective quantum yield of *D. salina*. The $\Delta F/F'_m$

Table 2 Photosynthetic parameters derived from the rapid light curves of *D. salina* acclimated to different $p\text{CO}_2$ levels

$p\text{CO}_2$	α	β	rETR _{max}	E_k
Control	0.211±0.005 ^a	0.400±0.091 ^a	75.5±2.7 ^a	357.9±4.6 ^a
1 000 μatm	0.239±0.002 ^b	0.434±0.056 ^a	90.8±2.8 ^b	379.2±9.3 ^a
2 000 μatm	0.233±0.01 ^b	0.521±0.082 ^a	96.2±9.0 ^b	412.6±23.1 ^b

Data shown are the means±SE ($n=3$). Different superscripted letters represent significant difference among the data.

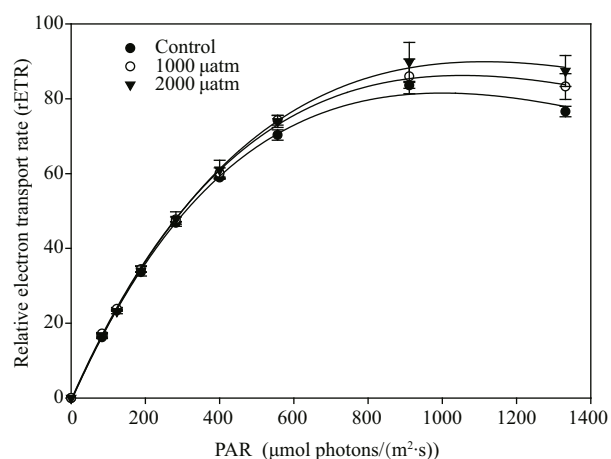


Fig.2 The rapid light curves of *D. salina* acclimated to different $p\text{CO}_2$ levels

Data shown are the means±SE ($n=3$).

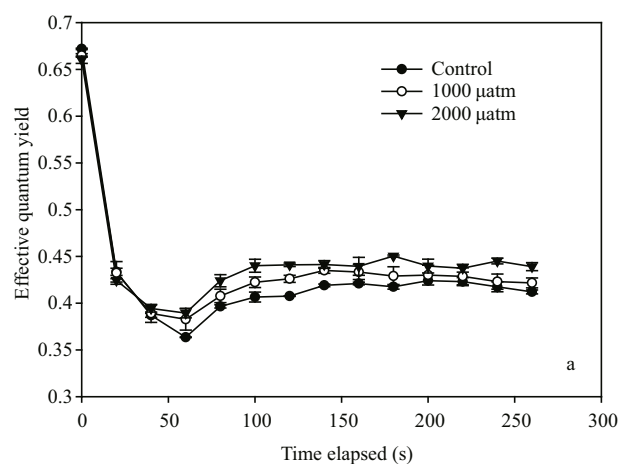


Fig.3 Effective quantum yield (yield) (a) and non-photochemical quenching (NPQ) (b) of *D. salina* acclimated to different $p\text{CO}_2$ levels

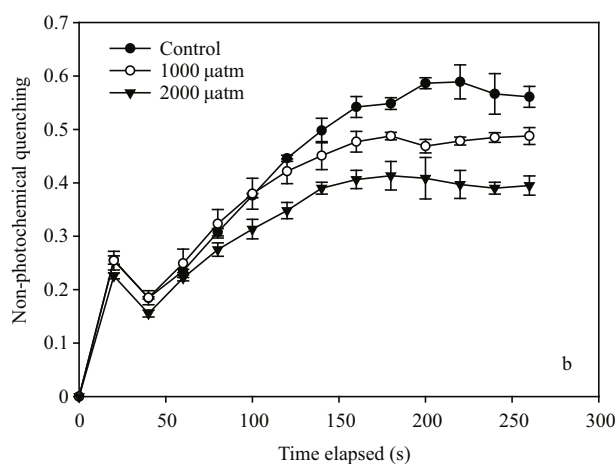
Data shown are the means±SE ($n=3$).

value was significantly stimulated by 2.2% ($P>0.05$) and 6.6% ($P<0.01$) under 1 000 and 2 000 μatm CO_2 relative to the control. Non-photochemical quenching (NPQ) showed a linear increase, then reached a plateau after 140 s. The cells acclimated to 1 000 and 2 000 μatm CO_2 showed a lower NPQ of about 86.6% ($P<0.01$) and 70.4% ($P<0.01$) of that in 390 μatm CO_2 (Fig.3b).

4.4 Photosynthetic oxygen evolution, dark respiration and Rubisco activities

The gross photosynthetic O_2 evolution (Fig.4b) was significantly enhanced by 14.65% ($P<0.05$) and 25.73% ($P<0.01$) under 1 000 and 2 000 μatm $p\text{CO}_2$, while elevated $p\text{CO}_2$ levels did not significantly influence the net photosynthetic O_2 evolution (Fig.4a) of *D. salina* ($P>0.05$). Similar to gross photosynthetic O_2 evolution, Rubisco activity (Fig.4d) was significantly stimulated by 23.86% ($P<0.05$) and 29.95% ($P<0.01$) under 1 000 and 2 000 μatm $p\text{CO}_2$. Cells acclimated to 2 000 μatm $p\text{CO}_2$ treatments showed a higher dark respiration rate than that of the control group ($P<0.05$), while there was no significant difference between the control group and the 1 000 μatm $p\text{CO}_2$ group ($P>0.05$) (Fig.4c).

The inhibitors AZ and EZ had significant effects on the photosynthetic O_2 evolution (Fig.5) of *D. salina* under different $p\text{CO}_2$ levels ($P<0.05$). The inhibitory effect was more pronounced at 390 μatm $p\text{CO}_2$ than at 1 000 and 2 000 μatm $p\text{CO}_2$. The inhibitory effect of AZ on the photosynthetic O_2 evolution of *D. salina* was 18.67% and 12.67% under 1 000 and 2 000 μatm $p\text{CO}_2$, respectively, which was significantly lower than that of 390 μatm $p\text{CO}_2$ ($P<0.05$), for which the



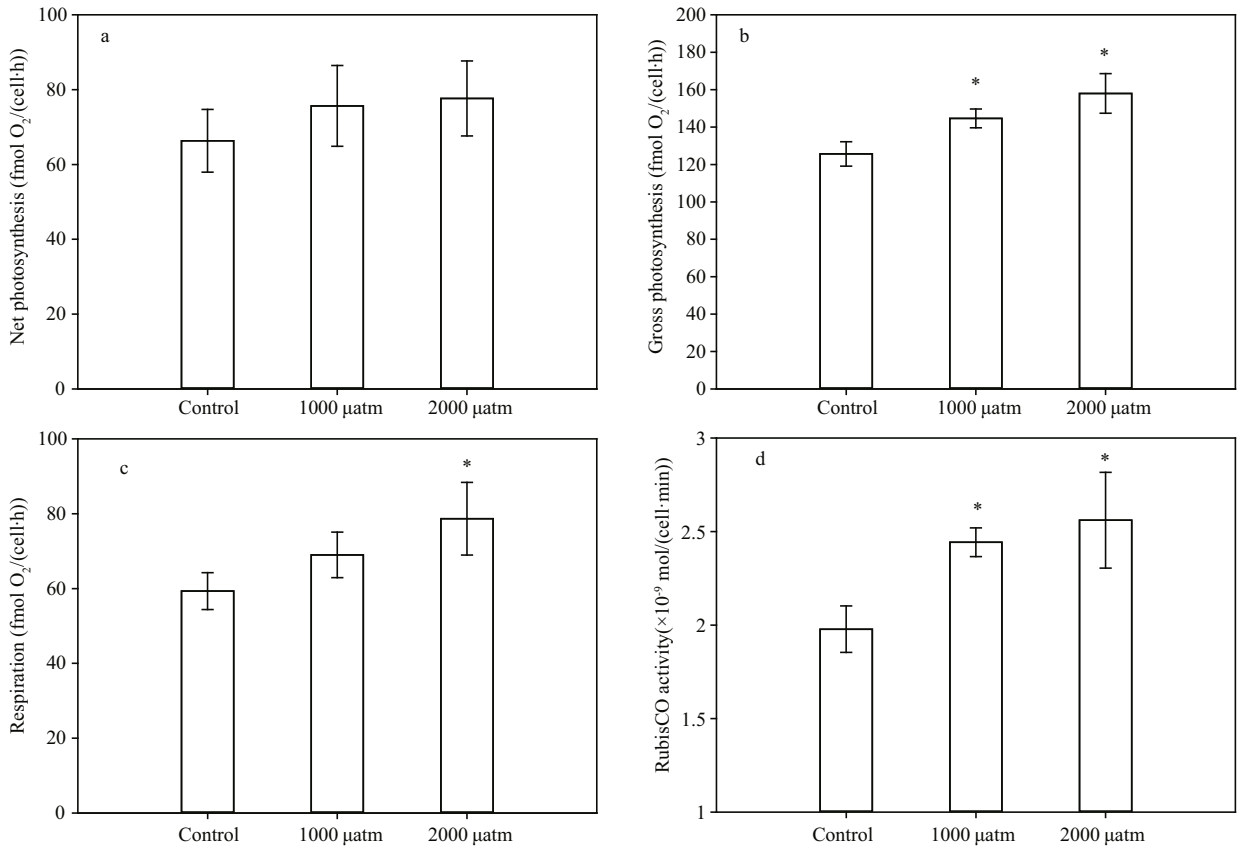


Fig.4 Net photosynthetic oxygen evolution (a), gross photosynthetic oxygen evolution (b), dark respiration (c) and RubisCO activity (d) of *D. salina* acclimated to different pCO₂ levels

Data are shown as the means±SE (n=3). The asterisks indicate significant differences with respect to the values of control cultures.

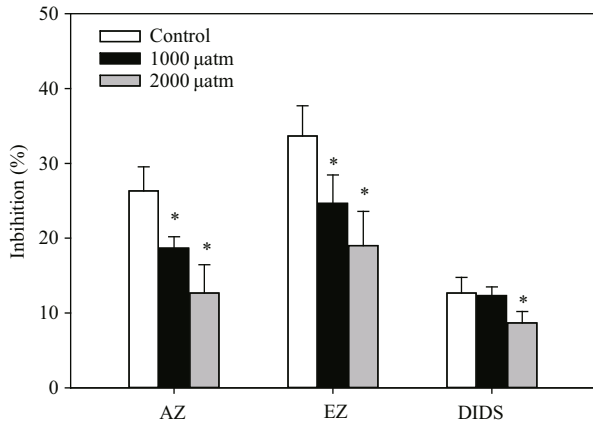


Fig.5 Inhibition rate of inhibitors (AZ, EZ and DIDS) on the photosynthetic O₂ evolution of *D. salina* under different pCO₂ levels

Data are shown as the means±SE (n=3). The asterisks indicate significant differences with respect to the values of control cultures.

inhibitory rate was 26.33%. The inhibitory rates of EZ were 24.67% and 19.10% under the two high pCO₂ treatments, respectively, while they were significantly lower than those obtained under 390 µatm pCO₂ (P<0.05). The inhibitory effects of DIDS on photosynthetic O₂ evolution of *D. salina* did

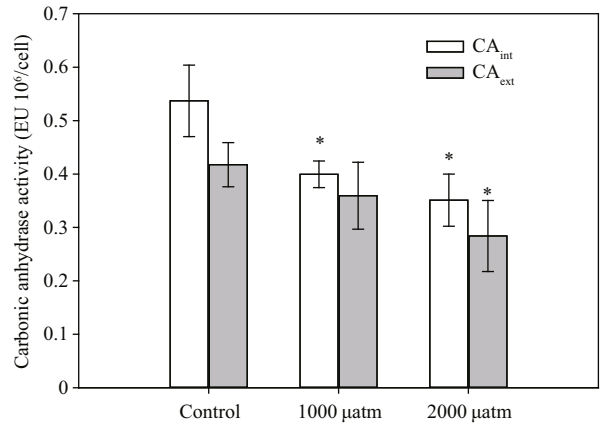


Fig.6 Carbonic anhydrase activity of *D. salina* acclimated to different pCO₂ levels

Data shown are the means±SE (n=3). The asterisks indicate significant differences with respect to the values of control cultures.

not differ significantly between the 390 and 1 000 µatm pCO₂ treatments (P>0.05), while the inhibitory effect of DIDS under 2 000 µatm pCO₂ was significantly lower than that of 390 µatm pCO₂.

4.5 Carbonic anhydrase

The carbonic anhydrase activities of *D. salina*

under different $p\text{CO}_2$ levels are shown in Fig.6. Relative to the control conditions, both the 1 000 μatm and 2 000 μatm $p\text{CO}_2$ groups showed significantly reduced internal carbonic anhydrase activity (CA_{int}), which decreased by 25.7% ($P<0.05$) and 34.6% ($P<0.01$), respectively. The external carbonic anhydrase activity (CA_{ext}) decreased significantly by 27.7% ($P<0.05$) when exposed to 2 000 μatm $p\text{CO}_2$ levels, while there was no significant difference between the 390 μatm and 1 000 μatm $p\text{CO}_2$ groups ($P>0.05$).

5 DISCUSSION

Different species of algae show different types of CCMs. The diatom *Thalassiosira pseudonana* (Yang and Gao, 2012), the diatom *Phaeodactylum tricorutum* (Burkhardt et al., 2001) and the chlorophyte *Chlorella ellipsoidea* (Matsuda and Colman, 1995) can use both CO_2 and HCO_3^- as a source of inorganic carbon, while the chlorophyte *Nannochloris atomus* (Huertas and Lubián, 1998) and the raphidophyceae *Heterosigma akashiwo* (Nimer et al., 1997) only use CO_2 . It is generally believed that CA_{ext} functions to increase the CO_2 concentration in the boundary layer by converting HCO_3^- to CO_2 , thereby facilitating CO_2 uptake. The presence of CCMs in *D. salina* is well established, and CA_{ext} plays an important role in the operation of CCMs (Booth and Beardall, 1991). In the present study, the net photosynthetic oxygen evolution of *D. salina* was significantly inhibited by acetazolamide (AZ) and 4,4'-diisothiocyano-stilbene-2,2'-disulfonate (DIDS), indicating that *D. salina* can use HCO_3^- via CA_{ext} and anion exchange (AE) protein. Furthermore, the operation of CCMs was down-regulated under high $p\text{CO}_2$ conditions, as indicated by the lower CA activity (CA_{ext} and CA_{int}) and the lower inhibition of the photosynthetic rate by AZ, EZ and DIDS (Fig.5) at high $p\text{CO}_2$. Such down-regulation of CCMs might be attributed to the elevated availability of CO_2 and HCO_3^- , as well as the increased entry of inorganic carbon into the cell by passive diffusion. Mercado et al. (1997) found that the CA_{int} activity of *Porphyra leucosticte* was significantly reduced at elevated $p\text{CO}_2$ levels, while the CA_{ext} activity was unaffected. Conversely, only the CA_{ext} activity of *Macrocystis pyrifera* was reduced when acclimated to 1 200 μatm CO_2 for 7 days, while the CA_{int} showed no significant changes (Fernández et al., 2015). These different responses to elevated CO_2 might be due to the different types of inorganic carbon uptake mechanisms in

different species and the contribution of CCMs to photosynthetic carbon fixation. Trimborn et al. (2009) showed that both CA_{ext} and CA_{int} activities of *T. pseudonana* are unaffected when acclimated to 800 μatm CO_2 for three days, while the CA_{int} activity and the photosynthetic affinity for CO_2 were lowered when the same strain was acclimated to 1 000 μatm CO_2 for 15 days (more than 20 generations) (Yang and Gao, 2012; Wu et al., 2015). The inconsistent results of the responses to elevated $p\text{CO}_2$ in the same strain might be due to the acclimation span or a different seawater carbonate system.

The long term cultivation experiment of *D. salina* under present and predicted future $p\text{CO}_2$ conditions showed that photosynthesis of *D. salina* was significantly influenced by CO_2 -induced ocean acidification in terms of rETR_{max} , $\Delta F/F'_m$, α and Rubisco activities. Moreover, the results indicated that the photosynthetic rate in this species is not saturated at present seawater inorganic carbon concentrations. The $\Delta F/F'_m$ of *D. salina* at high $p\text{CO}_2$ levels was significantly higher than that observed at the present $p\text{CO}_2$ levels. These results indicate that cells grown at high $p\text{CO}_2$ can use light more efficiently. The positive response of $\Delta F/F'_m$ to ocean acidification has also been reported for the rhodophyte *Neosiphonia harveyi* and the diatom *Navicula directa* (Torstensson et al., 2012; Olischläger and Wiencke, 2013). Generally, photosynthetic efficiency (α) represents light use efficiency (Fu et al., 2007, 2008). In *D. salina*, α in the control was significantly lower than in the high $p\text{CO}_2$ treatments, suggesting that future high $p\text{CO}_2$ levels increased the light use efficiency in *D. salina*. Moreover, Fu et al. (2007) proposed that an increased α at high $p\text{CO}_2$ is probably due to reduced energy allocation to the concentration CO_2 by the cell and for more efficient light use. The results of the present study support the conclusions of Fu et al. (2007), who found that elevated $p\text{CO}_2$ down-regulated the CCMs in *D. salina*, as indicated by decreased carbonic anhydrase activity and lowered inhibition of photosynthetic O_2 evolution by AZ, EZ and DIDS at high $p\text{CO}_2$. E_k ($\text{rETR}_{\text{max}}/\alpha$) represents the optimum light of the photosynthetic apparatus to maintain a balance between photosynthetic energy capture and the capacity to process this energy (Falkowski and Raven, 1997). Liu et al. (2012) reported that CO_2 -induced seawater acidification down-regulated CCMs in the green alga, *Ulva prolifera*, and that the subsequent energy savings contributed to a lower E_k . In the present study, although CCMs were also down-

regulated at high $p\text{CO}_2$ in *D. salina*, the energy saved did not lead to a lower E_k . On the contrary, increased E_k values at high $p\text{CO}_2$ were found in *D. salina*, probably due to stimulation of the maximal photosynthetic capacity ($r\text{ETR}_{\text{max}}$). Notably, the growth illumination of *D. salina* in our experiment was far below the E_k value, suggesting that *D. salina* was light-limited. The higher E_k at high $p\text{CO}_2$ indicates that the growth of *D. salina* under future conditions may be closely related to the availability of light, and that light is more likely to be a limiting factor for *D. salina* in the future. Conversely, the higher E_k at high $p\text{CO}_2$ also indicated that elevated $p\text{CO}_2$ led to a higher light threshold at which light becomes excessive, so that algae are less likely to experience light stress than under the present conditions.

Non-photochemical quenching (NPQ) is composed of energy-dependent quenching (qE), which is induced by acidification of the thylakoid lumen, state transition quenching (qT), which is concerned with the balance in the distribution of excitation energy between the two photosystems, and photoinhibitory quenching (qI), which is related to photo-inhibition of photosynthesis (Krause and Jahns, 2004). In the present study, CO_2 -induced ocean acidification significantly decreased the NPQ of *D. salina* (Fig.3b). The synthesis of ATP will lead to translocation of the hydrogen ion from the thylakoid lumen to the stroma, thus weakening the acidification of the thylakoid lumen. Because enhanced carboxylation (Fig.4d) at high $p\text{CO}_2$ requires more ATP, more H^+ ions are transported out of the thylakoid lumen, leading to decreased qE. However, cyclic electron transports, which play an important role in photo-protection by producing and maintaining the ΔpH , can be accelerated by the operation of CCMs (Heimann and Schreiber 1999). Down-regulated CCMs of *D. salina* can reduce cyclic electron transport (Moroney and Somanchi, 1999), leading to increased qI. Thus, the response of NPQ to elevated $p\text{CO}_2$ appears to reflect the net effects of a decreased qE and an increased qI.

Ribulose-1,5-bisphosphate carboxylase/oxygenase (Rubisco) catalyzes the first step in photosynthetic carbon fixation and is the rate-limiting reaction of the Calvin cycle (Spreitzer and Salvucci, 2002). In the present study, increased Rubisco activity at high $p\text{CO}_2$ indicated that elevated $p\text{CO}_2$ enhanced the photosynthetic carbon fixation in *D. salina* (Fig.4d). Similar to the trend in rubisco activity, high $p\text{CO}_2$ conditions enhanced dark respiration in *D. salina* (Fig.4c), indicating a higher energy requirement due

to either enhanced biosynthesis in response to increased photosynthetic carbon fixation or increased energy requirements to maintain the intracellular acid-base stability (Geider and Osborne, 1989). The enhanced dark respiration would consume more gross photosynthetic production under future high $p\text{CO}_2$ and low pH conditions (del Giorgio and Duarte, 2002). Therefore, the unchanged growth of *D. salina* could be attributed to the balance of the stimulated carbon assimilation and carbon loss. Similar to *D. salina*, enhanced photosynthesis and respiration were found in the diatom *Thalassiosira pseudonana*, while growth was not significantly affected by high $p\text{CO}_2$ (Yang and Gao, 2012). Stimulated photosynthesis and growth were found in *Phaeodactylum tricorutum*, *Ulva prolifera* and *Heterosigma akashiwo* (Fu et al., 2008; Wu et al., 2010; Xu and Gao, 2012) under high $p\text{CO}_2$ conditions, since energy was saved in down-regulated CCMs or when there was enhanced availability of CO_2 . However, many other studies have shown no significant effects (Fu et al., 2008; Fernández et al., 2015), and even negative effects (Gao et al., 2012; Iñiguez et al., 2016) on the growth and photosynthesis of marine phytoplankton. These studies, together with our results, indicate that the different responses of marine phytoplankton to CO_2 -induced ocean acidification might be related to the net outcome of the positive and negative (extra carbon loss) effects, although the diverse mechanisms of inorganic carbon acquisition and other environmental factors might affect the responses of marine algae to elevated $p\text{CO}_2$.

It has been widely reported that other environmental factors, such as light intensity, temperature and nutrient supply, might modulate the response of algae to increased $p\text{CO}_2$. Gao et al. (2012) found that stimulated growth of *P. tricorutum*, *T. pseudonana* and *Skeletonema costatum* under high $p\text{CO}_2$ levels was observed under low light levels, whereas a reverse trend was observed at high light levels. Similarly, different light intensity and nitrogen levels modulated the effects of $p\text{CO}_2$ on *Gracilaria lemaneiformis* (Zou and Gao, 2009; Zou et al., 2011). The PSP toxin content of *Alexandrium fundyense* decreased with elevated $p\text{CO}_2$ under N-limited conditions, while it showed an adverse trend under N-replete conditions (Eberlein et al., 2016). For *H. akashiwo*, the effects of $p\text{CO}_2$ on the growth rate were dependent on temperature, with a positive effect observed at 20°C and no effect observed at 24°C (Fu et al., 2008). For the red algae *Chondrus crispus*, a

significant effect of elevated $p\text{CO}_2$ on photosynthesis and growth was only observed in interactions with either high temperature or reduced light levels (Sarker et al., 2013). Overall, the results of these studies indicate how changeable and complicated the response of *D. salina* to the predicted future ocean might be, and that this response might be modulated by experimental conditions.

6 CONCLUSION

Based on the results of the present study, CO_2 -induced ocean acidification might lead *D. salina* to enhance photosynthesis, down-regulate their CCMs, and stimulate dark respiration, resulting in an unchanged growth rate. The net effect of ocean acidification on microalgae will be determined by the balance of these positive and negative effects. However, further studies are needed to evaluate the interactive effects of $p\text{CO}_2$, light, nutrients and temperature on growth, photosynthesis and other physiological processes to determine how this species might respond to future ocean conditions.

7 ACKNOWLEDGMENT

We thank all of the members of the laboratory and Dr. LIANG in the College of Fisheries of Ocean University of China for their help.

References

Axelsson L, Ryberg H, Beer S. 1995. Two modes of bicarbonate utilization in the marine green macroalga *Ulva lactuca*. *Plant Cell Environ.*, **18**(4): 439-445.

Badger M R, Andrews T J, Whitney S M, et al. 1998. The diversity and coevolution of Rubisco, plastids, pyrenoids, and chloroplast-based CO_2 -concentrating mechanisms in algae. *Can J Bot.*, **76**(6): 1 052-1071.

Booth W A, Beardall J. 1991. Effects of salinity on inorganic carbon utilization and carbonic anhydrase activity in the halotolerant alga *Dunaliella salina* (Chlorophyta). *Phycologia*, **30**(2): 220-225.

Burkhardt S, Amoroso G, Riebesell U, Sültemeyer D. 2001. CO_2 and HCO_3^- uptake in marine diatoms acclimated to different CO_2 concentrations. *Limnol. Oceanogr.*, **46**(6): 1 378-1 391.

Caldeira K, Wickert M E. 2003. Oceanography: anthropogenic carbon and ocean pH. *Nature*, **425**(6956): 365.

del Giorgio P A, Duarte C M. 2002. Respiration in the open ocean. *Nature*, **420**(6914): 379-384.

Eberlein T, van de Waal D B, Brandenburg K M, John U, Voss M, Achterberg E P, Rost B. 2016. Interactive effects of ocean acidification and nitrogen limitation on two bloom-forming dinoflagellate species. *Mar. Ecol. Prog. Ser.*,

543: 127-140.

Falkowski P G, Raven J A. 2013. Aquatic Photosynthesis. Princeton University Press, Princeton.

Fernández P A, Roleda M Y, Hurd C L. 2015. Effects of ocean acidification on the photosynthetic performance, carbonic anhydrase activity and growth of the giant kelp *Macrocystis pyrifera*. *Photosynth. Res.*, **124**(3): 293-304.

Fu F X, Warner M E, Zhang Y H, Feng Y Y, Hutchins D A. 2007. Effects of increased temperature and CO_2 on photosynthesis, growth, and elemental ratios in marine *Synechococcus* and *Prochlorococcus* (Cyanobacteria). *J. Phycol.*, **43**(3): 485-496.

Fu F X, Zhang Y H, Warner M E, Feng Y Y, Sun J, Hutchins D A. 2008. A comparison of future increased CO_2 and temperature effects on sympatric *Heterosigma akashiwo* and *Prorocentrum minimum*. *Harmful Algae*, **7**(1): 76-90.

Gao K S, Xu J T, Gao G, Li Y H, Hutchins D A, Huang B Q, Wang L, Zheng Y, Jin P, Cai X N, Häder D P, Li W, Xu K, Liu N N, Riebesell U. 2012. Rising CO_2 and increased light exposure synergistically reduce marine primary productivity. *Nat. Climate Change*, **2**(7): 519-523.

Geider R J, Osborne B A. 1989. Respiration and microalgal growth: a review of the quantitative relationship between dark respiration and growth. *New Phytol.*, **112**(3): 327-341.

Gerard V A, Driscoll T. 1996. A spectrophotometric assay for rubisco activity: application to the kelp *Laminaria saccharina* and implications for radiometric assays1. *J. Phycol.*, **32**(5): 880-884

Giordano M, Beardall J, Raven J A. 2005. CO_2 concentrating mechanisms in algae: mechanisms, environmental modulation, and evolution. *Annu. Rev. Plant Biol.*, **56**(1): 99-131.

Giordano M, Maberly S C. 1989. Distribution of carbonic anhydrase in British marine macroalgae. *Oecologia.*, **81**(4): 534-539.

Guillard R R L. 1975. Culture of phytoplankton for feeding marine invertebrates. In: Smith W L, Chanley M H eds. Culture of Marine Invertebrate Animals. Springer, New York, USA. p.29-60

Guinotte J M, Fabry V J. 2008. Ocean acidification and its potential effects on marine ecosystems. *Ann. N. Y. Acad. Sci.*, **1134**(1): 320-42.

Heimann S, Schreiber U. 1999. Cyt b-559 (Fd) participating in cyclic electron transport in spinach chloroplasts: evidence for kinetic connection with the cyt b6/f complex. *Plant Cell Physiol.*, **40**(8): 818-824.

Huertas I E, Lubián L M. 1998. Comparative study of dissolved inorganic carbon utilization and photosynthetic responses in *Nannochloris* (chlorophyceae) and *Nannochloropsis* (eustigmatophyceae) species. *Can. J. Bot.*, **76**(6): 1 104-1 108.

Hutchins D A, Fu F X, Zhang Y, Warner M E, Feng Y, Portune K, Bernhardt P W, Mulholland M R. 2007. CO_2 control of *Trichodesmium* N_2 fixation, photosynthesis, growth rates, and elemental ratios: Implications for past, present, and future ocean biogeochemistry. *Limnol. Oceanogr.*, **52**(4):

- 1 293-1 304.
- Ihnken S, Roberts S, Beardall J. 2011. Differential responses of growth and photosynthesis in the marine diatom *Chaetoceros muelleri* to CO₂ and light availability. *Phycologia*, **50**(2): 182-193.
- Iñiguez C, Carmona R, Lorenzo M R, Niell F X, Wiencke C, Gordillo F J L. 2016. Increased CO₂ modifies the carbon balance and the photosynthetic yield of two common arctic brown seaweeds: *Desmarestia aculeata* and *Alaria esculenta*. *Polar Biol.*, **39**(11): 1 979-1 991.
- Iñiguez C, Lorenzo M R, Niell F X, Wiencke C, Gordillo F J, Carmona Fernández R. 2015. Effects of increased CO₂ in the carbon budget and the photosynthetic yield of the arctic seaweeds *Alaria esculenta* and *Desmarestia aculeata*. <http://hdl.handle.net/10630/9265>.
- IPCC. 2013. Climate Change 2013: the physical science basis. In: Stocker TF, Qin D, Plattner GK, Tignor M, Allen SK, Boschung J, Nauels A, Xia Y, Bex V, Midgley P M eds. Contribution of working group I to the fifth assessment report of the intergovernmental panel on climate change. Cambridge University Press, Cambridge. p.1 535.
- Kranz S A, Dieter S, Richter K U, Rost B. 2009. Carbon acquisition by *Trichodesmium*: the effect of pCO₂ and diurnal changes. *Limnol. Oceanogr.*, **54**(2): 548-559.
- Krause G H, Jahns P. 2004. Non-photochemical energy dissipation determined by chlorophyll fluorescence quenching: characterization and function. In: Papageorgiou G C, Govindjee eds. Chlorophyll a Fluorescence. Springer, Netherlands. p.463-495
- Kurihara H, Asai T, Kato S, Ishimatsu A. 2008. Effects of elevated pCO₂ on early development in the mussel *Mytilus galloprovincialis*. *Aquat. Biol.*, **4**(3): 225-233.
- Langer G, Geisen M, Baumann K H, Kläs J, Riebesell U, Thoms S, Young J R. 2006. Species-specific responses of calcifying algae to changing seawater carbonate chemistry. *Geochem. Geophys. Geosyst.*, **7**(9): 535-540.
- Lewis E, Wallace D, Allison L J. 1998. Program developed for CO₂ system calculations. Tennessee: Carbon Dioxide Information Analysis Center, Oak Ridge National Laboratory, US Department of Energy.
- Liu Y T, Xu J T, Gao K S. 2012. CO₂-driven seawater acidification increases photochemical stress in a green alga. *Phycologia*, **51**(5): 562-566.
- Liu Z Y, Zhang L J, Cai W J, Wang L, Xue M, Zhang X S. 2014. Removal of dissolved inorganic carbon in the yellow river estuary. *Limnol. Oceanogr.*, **59**(2): 413-426.
- Matsuda Y, Colman B. 1995. Induction of CO₂ and bicarbonate transport in the green alga *Chlorella ellipsoidea* (II. Evidence for induction in response to external CO₂ concentration). *Plant Physiol.*, **108**(1): 253-260.
- Mercado J M, Javier F, Gordillo L, Niell F X, Figueroa F L. 1999. Effects of different levels of CO₂ on photosynthesis and cell components of the red alga *Porphyra leucosticta*. *J. Appl. Phycol.*, **11**(5): 455-461.
- Mercado J M, Niell F X, Figueroa F L. 1997. Regulation of the mechanism for HCO₃⁻ use by the inorganic carbon level in *Porphyra leucosticta* Thur. in Le Jolis (Rhodophyta). *Planta*, **201**(3): 319-325.
- Moroney J V, Husic H D, Tolbert N E. 1985. Effect of carbonic anhydrase inhibitors on inorganic carbon accumulation by *Chlamydomonas reinhardtii*. *Plant Physiol.*, **79**(1): 177-183.
- Moroney J V, Somanchi A. 1999. How do algae concentrate CO₂ to increase the efficiency of photosynthetic carbon fixation?. *Plant Physiol.*, **119**(1): 9-16.
- Nimer N A, Iglesias-Rodríguez M D, Merrett M J. 1997. Bicarbonate utilization by marine phytoplankton species. *J. Phycol.*, **33**(4): 625-631.
- Olischläger M, Wiencke C. 2013. Ocean acidification alleviates low-temperature effects on growth and photosynthesis of the red alga *Neosiphonia harveyi* (rhodophyta). *J. Exp. Bot.*, **64**(18): 5 587-5 597.
- Platt T, Gallegos C L, Harrison W G. 1980. Photoinhibition of photosynthesis in natural assemblages of marine phytoplankton. *J. Mar. Res.*, **38**: 687-701.
- Ralph P J, Gademann R. 2005. Rapid light curves: a powerful tool to assess photosynthetic activity. *Aquat. Bot.*, **82**(3): 222-237.
- Reinfeldt J R. 2011. Carbon concentrating mechanisms in eukaryotic marine phytoplankton. *Annu. Rev. Mar. Sci.*, **3**(1): 291-315.
- Riebesell U, Schulz K G, Bellerby R G J, Botros M, Fritsche P, Meyerhöfer M, Neill C, Nondal G, Oschlies A, Wohlers J, Zöllner E. 2007. Enhanced biological carbon consumption in a high CO₂ ocean. *Nature*, **450**(7169): 545-548.
- Rost B, Richter K U, Riebesell U, Hansen P J. 2006. Inorganic carbon acquisition in red tide dinoflagellates. *Plant Cell Environ.*, **29**(5): 810-822.
- Rost B, Riebesell U, Burkhardt S, Sültemeyer D. 2003. Carbon acquisition of bloom-forming marine phytoplankton. *Limnol. Oceanogr.*, **48**(1): 55-67.
- Sarker M Y, Bartsch I, Olischläger M, Gutow L, Wiencke C. 2013. Combined effects of CO₂, temperature, irradiance and time on the physiological performance of *Chondrus crispus* (Rhodophyta). *Bot. Mar.*, **56**(1): 63-74.
- Spreitzer R J, Salvucci M E. 2002. RUBISCO: structure, regulatory interactions, and possibilities for a better enzyme. *Annu. Rev. Plant Biol.*, **53**(1): 449-475.
- Torstensson A, Chierici M, Wulff A. 2012. The influence of increased temperature and carbon dioxide levels on the benthic/sea ice diatom *Navicula directa*. *Polar Biol.*, **35**(2): 205-214.
- Trimborn S, Lundholm N, Thoms S, Richter K U, Krock B, Hansen P J, Rost B. 2008. Inorganic carbon acquisition in potentially toxic and non-toxic diatoms: the effect of pH-induced changes in seawater carbonate chemistry. *Physiol Plant*, **133**(1): 92-105.
- Trimborn S, Wolf-Gladrow D, Richter K U, Rost B. 2009. The effect of pCO₂ on carbon acquisition and intracellular assimilation in four marine diatoms. *J. Exp. Mar. Biol. Ecol.*, **376**(1): 26-36.
- Van de Waal D B, John U, Ziveri P, Reichart G J, Hoins M, Sluijs A, Rost B. 2013. Ocean acidification reduces growth and calcification in a marine dinoflagellate. *PLoS*

- One*, **8**(6): e65987.
- Wellburn A R. 1994. The spectral determination of chlorophylls *a* and *b*, as well as total carotenoids, using various solvents with spectrophotometers of different resolution. *J. Plant Physiol.*, **144**(3): 307-313.
- Wu Y P, Beardall J, Gao K S. 2015. Physiological responses of a model marine diatom to fast pH changes: special implications of coastal water acidification. *PLoS One*, **10**(10): e0141163.
- Wu Y, Gao K, Riebesell U. 2010. CO₂-induced seawater acidification affects physiological performance of the marine diatom *Phaeodactylum tricorutum*. *Biogeosciences*, **7**(9): 2 915-2 923.
- Xu J T, Gao K S. 2012. Future CO₂-induced ocean acidification mediates the physiological performance of a green tide alga. *Plant Physiol.*, **160**(4): 1 762-1 769.
- Yang G Y, Gao K S. 2012. Physiological responses of the marine diatom *Thalassiosira pseudonana* to increased pCO₂ and seawater acidity. *Mar. Environ. Res.*, **79**: 142-151.
- Zhang X X, Tang X X, Zhou B, Hu S X, Wang Y. 2015. Effect of enhanced UV-B radiation on photosynthetic characteristics of marine microalgae *Dunaliella salina* (Chlorophyta, Chlorophyceae). *J. Exp. Mar. Biol. Ecol.*, **469**: 27-35.
- Zou D H, Gao K S, Luo H J. 2011. short- and long-term effects of elevated CO₂ on photosynthesis and respiration in the marine macroalga *Hizikia fusiformis* (Sargassaceae, Phaeophyta) grown at low and high N supplies. *J. Phycol.*, **47**(1): 87-97.
- Zou D H, Gao K S. 2009. Effects of elevated CO₂ on the red seaweed *Gracilaria lemaneiformis* (Gigartinales, Rhodophyta) grown at different irradiance levels. *Phycologia*, **48**(6): 510-517.